THOMPSON, M. J., AND R. T. WOLCOTT. 1976. Remote sensing services. Pp. 5-19. *In*: Young, D. K. (ed.). Harbor Branch Foundation, Inc., Indian River Coastal Zone Study, Annual Report, 1975-1976. Harbor Branch Foundation, Inc., Ft. Pierce.

WHITFIELD, M. 1969. Eh as an operational parameter in estuarine studies. Limnol. Oceanogr. 14:527-558.

Academy Symposium

COMPUTER SIMULATION OF LIGHT ATTENUATION

WILLIAM A. HOGAN[1]

Department of Engineering Sciences, Florida Institute of Technology, Jensen Beach, Florida 33457

ABSTRACT: *A computer simulation model developed to study light attenuation in the ocean was applied to clear, medium turbid and turbid waters under diverse conditions. The model theory is based upon multiple small angle scattering of photons by hydrosols and molecules, and includes the effects of absorption. Results show a striking difference between clear and turbid waters and demonstrate the strong dependence of transmittance on turbidity.*

THE subject of underwater optics is of importance to those interested in oceanic photosynthesis and its effects on various biological problems. A discrete particle simulation technique, developed for modeling non-linear processes in physics (Hogan and Stetson, 1975) was used to investigate downward photon scattering in ocean systems. The technique is presented as a simple alternative to the Monte Carlo method (Kattawar et al., 1973 and Gordon, 1976). The technique has also been successfully applied to study reaction-diffusion in chemical and biological systems (Stetson et al., 1976 and Hogan and Stetson, 1982). The model simulated Rayleigh scattering of photons by water molecules, Mie scattering off hydrosols, and included radiant energy losses due to absorption. The scattering of photons at angles of 0° to 90° was investigated, but the contribution due to backscattering was not included. The parameters for the model were chosen to be in agreement with data gathered in the St. Lucie Inlet and surrounding coastal waters. Downward scattering was calculated as a function of photon wavelength, the size and density of suspended particulate matter, and the depth in the medium.

METHODS— The model assumed that for radiance calculations, photons can be treated as discrete "particles" and that multiple small angle scattering predominates. Consequently, the Mie and Raleigh scattering functions were treated independently and sequentially, the incident radiation was taken to be plane electromagnetic waves with random polarization, and the effects of interference were not included. The model simulated smooth ocean surface water with the

[1]Present Address: Harris Corporation, Computer Systems Division, Ft. Lauderdale, Florida 33901.

solar angle at the zenith, and did not consider the effects of ocean floor albedo. The suspended particulate matter was assumed spherical and the distribution was assumed homogeneous and isotropic. The simulation was for ocean surface waters, the average temperature of the medium was 20°C, and the refractive index was taken to be 1.34 for the ocean water and 1.20 for the particles.

The basic simulation scheme had 4 sequential portions. An initial uniform distribution of one million monochromatic photons was incident upon the test volume of the computer simulated ocean water. The photons travelled downward in steps of 1 m, $\triangle z = 1$, and the resulting angular distribution was calculated. At each step the photons were first Mie scattered by the hydrosols then Rayleigh scattered by the water molecules. Next, the fraction of photons lost due to absorption was subtracted from the total number remaining at that depth and a new angular distribution was calculated for the photons. The process was repeated until the photons reached a depth of 10 m. The simulation was performed for 5 wavelengths covering the visible spectrum using the clear ocean model, and for blue light using the medium and turbid ocean models.

The simulation technique used statistical weights to determine relative effects of the attenuation processes. Three cross section ratios specify these processes (Kattawar et al., 1973). The ratio CRS determines the probability that a photon is Rayleigh scattered instead of Mie scattered, the ratio CMS determines the probability that a photon is Mie scattered instead of Rayleigh scattered, and CTS determines the probability that a photon is scattered instead of being absorbed upon collision. Table 1 gives these probabilities as a function of wavelengths for clear ocean

TABLE 1. Cross section ratios for photon scattering as a function of wavelength and turbidity.

Wavelength (nm)	Water	CRS	CMS	CTS
400	Clear	.328	.672	.555
460	Clear	.218	.782	.514
480	Clear	.190	.810	.491
500	Clear	.166	.834	.447
550	Clear	.120	.880	.332
650	Clear	.065	.935	.080
460	Medium	.079	.921	.380
460	Turbid	.045	.955	.270

water and gives them for blue light in medium turbid and turbid waters. Water is considered clear when approximately 50% or less of the incident light is absorbed in the first meter of penetration. The water is medium turbid for approximately 60% absorption and turbid for approximately 70% absorption.

The Mie scattering (hydrosol) portion of the simulation was performed by first multiplying the total number of photons by CMS to determine what fraction of the downward flux underwent particle scattering. The angular distribution of the photons thus scattered was calculated using a random walk probability function. The probability that a photon will be scattered through an angle Θ is given by:

$$P(\Theta) = (2 \pi\sigma)^{-1/2} \exp(- \Theta^2/2\sigma)$$

where σ is the mean-square scattering angle. It has been shown (Modesit, 1971) that

$$\sigma = N\pi zR^2(n-n_e)^2/n_e^2$$

where N is the number density of particles per m^3, z is the distance in m travelled per step, R is the avg particle radius in m, n is the refractive index for the particles, and n_e is the refractive index for the ocean water. By varying these parameters in σ it is possible to simulate different types of ocean water.

The Rayleigh scattering (molecular) portion of the simulation was performed by multiplying the number of photons by CRS to determine the fraction that are scattered by the water molecules. The angular distribution of these photons was calculated using the scattering function

for seawater given by Morel (1974). The function coefficients bring into account the strong dependence of scattering on wavelength, which is inversely proportional to the fourth power of the wavelength. Morel's function also accounted for the effects of pressure on the relative index of refraction by shifting the exponent from 4.0 to 4.32.

Losses due to absorption were incorporated by multiplying the number of photons scattered into each angular direction by CTS. When the statistical weight of a photon became less than 10^{-6} it was subtracted from the distribution of downward flux and was no longer considered.

This completed 1 iterative cycle. The resulting angular distribution of photons was calculated and a graph of the intensity versus angle was printed. The next step was to increment the depth by one meter and then repeat the entire process. Using this procedure the photons were followed to a depth of 10 m.

The parameters for the model were chosen to agree with data gathered in the mouth of the St. Lucie Inlet and surrounding coastal waters (Florida Institute of Technology, 1981). The logic behind the choice of parameters was to provide a simulation study of the waters near the inlet prior to the 1981 dredging project. Secchi disk measurements and submarine photometer readings indicated that these waters could be considered medium turbid, on the average, for the period of the study. The parameters chosen were consistent with data gathered in the Ft. Pierce Inlet (Thompson et al., 1979. For comparison, the computer model was run using cross section probabilities for clear, medium turbid and turbid waters. Other parameters chosen for this model were:

$$\text{Average temperature} = 20°C$$

$$\text{Average particle radius} = 3 \times 10^{-6}\text{m}$$

$$\text{Average particle density} = 2 \times 10^{7}\text{m}^{-3}$$

A convenient feature of this model is that these parameters can be easily modified to simulate other experimental data.

RESULTS — Fig. 1 shows results for the clear water model where photon intensity is plotted against scattering angle at a depth of 10 m. The 5 curves
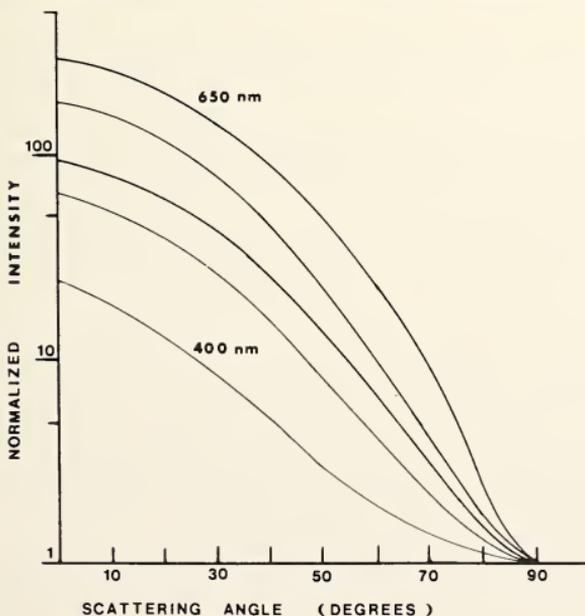

FIG. 1. Photon intensity vs. scattering angle at a depth of 10 m in clear ocean water. The curves are for wavelengths of 650 nm, 550 nm, 500 nm, 460 nm, and 400 nm.
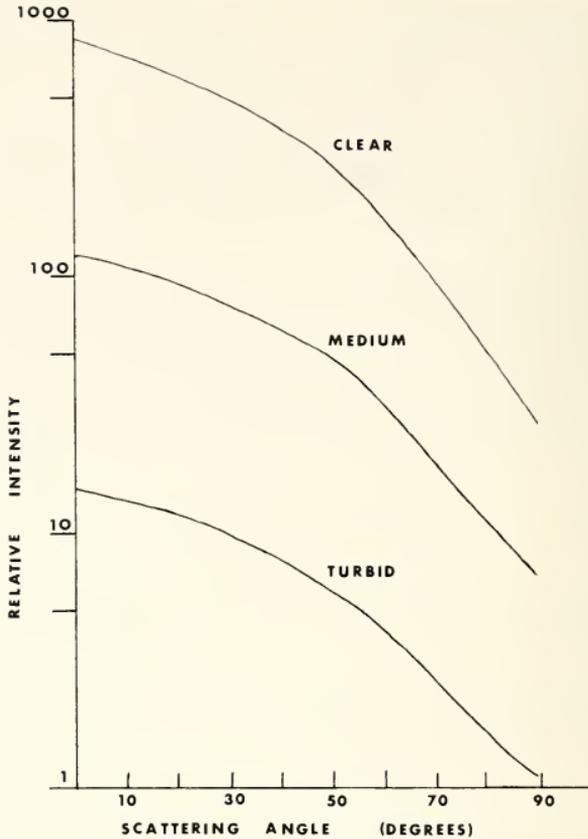
FIG. 2. Photon intensity vs. scattering angle at a depth of 6 m. The results are for clear, medium turbid and turbid waters at a wavelength of 460 nm.

represent wavelengths of 650 nm, 550 nm, 500 nm, 460 nm, and 400 nm. This clearly demonstrates the dependence of attenuation upon wavelength. Data were normalized to the scattering at 90° to illustrate the differentiation at small angles and plotted on semi-log paper.

Fig. 2 shows the dramatic differences among the clear, medium turbid and turbid waters. Results are for blue light (460 nm) at a depth of 6 m, where the relative intensity is plotted against scattering angle. It is evident that transmittance decreases as the turbidity increases. Photon intensity was decreased by a factor of 0.14 for medium turbid water and by a factor of 0.02 for turbid water, compared to clear water at the same depth. The model also indicated that maximum transmittance shifted towards the red end of the spectrum as turbidity increased.

Fig. 3 illustrates the sensitivity of the model to changes in particle density and particle radius. Curve A is the same as the one shown in Fig. 2 for medium turbid water at a depth of 6 m. Curve B is obtained when the particle density was changed from 2×10^7 to $4 \times 10^7 \text{m}^{-3}$, and curve C is obtained
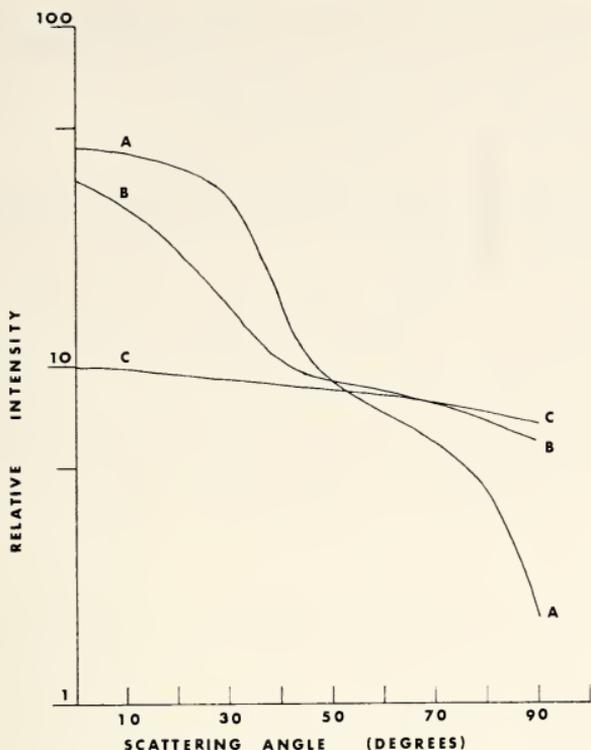
FIG. 3. Photon intensity vs. scattering angle at a depth of 6 m. For curve B the particle radius was twice that for curve A and for curve C the particle density was doubled. Results are for medium turbid water at a wavelength of 460 nm.

when the particle radius was changed from 3 x 10⁻⁶m to 6 x 1-⁻⁶m. All other parameters were held constant for these comparisons. Results indicate that when either the density or radius was increased, the photon intensity decreased at small scattering angles and increased at larger angles.

CONCLUSION — Absorption dominates the attenuation of electromagnetic radiation except in the narrow range of the visible spectrum. Scattering becomes an important contribution to the total attenuation in the 350 nm to 500 nm range. In clear ocean water approximately 50 % of the radiation is absorbed in the first m of penetration as a result of the extinction of the infrared. Maximum transmission is at about 465 nm (blue-green) in clear water and shifts to higher wavelengths (about 550 nm) in turbid water. This observed shift results because the suspended particulate matter both absorbs and scatters shorter wavelengths more than longer wavelengths. Another contributing factor is that dissolved organic material selectively absorbs shorter wavelengths. The final result is that maximum transmittance shifts towards longer wavelengths in the more turbid coastal waters, and total transmittance decreases.

Future investigations should include additional computer simulations on

light attenuation as new data become available on particle size, density and turbidity in the St. Lucie Inlet and surrounding coastal waters.

LITERATURE CITED

FLORIDA INSTITUTE OF TECHNOLOGY, OCEANOGRAPHIC TECHNOLOGY DIVISION. 1981. Data gathered on student training cruises from September 1978 through May 1981.

GORDON, H. 1976. Radioactive transfer in the oceans. Appl. Optics. 15:2611-2613.

HOGAN, W., AND R. STETSON. 1975. Hot-ion distribution studies in a mirror contained plasma. Plasma Physics. 17:773-783.

_____. 1982. Simulation of chemical oscillation in a membrane. Bull. Math. Bio. 44: 637-645.

KATTAWAR, J., G. PLASS, AND J. GUINN. 1973. Monte Carol calculations of polarization of radiation in the Earth's atmosphere-ocean system. J. Phys. Ocean. 3:353-372.

MOREL, A. 1974. Optical aspects of oceanography. P. 19. *In*: Jerlow, N., and E. Nielson (ed.). Academic Press, New York.

STETSON, R., J. MCGUIRE, AND W. HOGAN. 1976. Simulation of non-linear reaction diffusion equations. Bull. Math. Bio. 39:391-396.

THOMPSON, M., L. GILLILAND, AND L. ROSENFELD. 1979. Light scattering and extinction in a highly turbid coastal inlet. Estuaries. 2:164-171.

Academy Symposium

THE OCCURRENCE OF A TOXIC DINOFLAGELLATE IN THE INDIAN RIVER SYSTEM

D. R. NORRIS

Department of Oceanography and Ocean Engineering,
Florida Institute of Technology, Melbourne, Florida 32901

ABSTRACT: *References to the toxic dinoflagellate,* Gonyaulax monilata *Howell, in the Indian and Banana rivers are compiled from published and unpublished sources. The inability of researchers to find motile cells for extended periods indicates that benthic resting cysts or hypnozygotes may be the only source for the seed population.*

GONYAULAX MONILATA Howell was originally described from red tides in the Banana and Indian rivers in 1951 (Howell, 1953). Howell reported that water discoloration was caused by large numbers of dinoflagellates, but no great quantity of fish were killed. *G. monilata* was taken "from all stations in the Indian and Banana Rivers" but no reference was given for specific station locations. Although there have been numerous "red tides" and fish kills in this lagoonal system over the last 30 yr, there is no published record of *G. monilata* presence. I compiled the references to this species which to date

were only in laboratory notes (C. Down, Brevard County Health Department, B.C.H.D.) or in theses (Modert, 1977; Trees, 1977; Donnelly, 1980) from Florida Institute of Technology, in addition to the paper by Howell (1953). Additional comment is made regarding the absence of this species in the estuary.

TABLE 1. Occurrence of motile *Gonyaulax monilata* in the Indian River lagoon system.

Date	Location, Comment and Source	Cells/Liter	Dissolved Oxygen (ppm)	Temp. (°C)	Sal. ($^o/_{oo}$)
Aug- Sept 1951	"Indian & Banana Rivers: (discolored water, minor fish kill). Howell, 1953	"Large Nos."	-	30-34	18-32
12 July 1977	Between Eau Gallie & Melbourne Causeways (No fish kill). Trees, 1977	8.9×10^5	-	31.5-32	32.0
27 July 1977	Melbourne Beach Pier (no fish kill). Modert, 1977	$1.7 \times 10^{6*}$	6.0	29.5	30.5
9 Sept 1977	W-Side of I.R., Port St. John (1000's dead fish) B.C.H.D. (unpubl.)	"Bloom"	"Depleted"	-	-
6 Sept 1979	Scattered from Horse Cr. to Fisherman Point (no fish kill) Donnelly, 1980	$< 1.0 \times 10^3$	4.8-7.6	24.5-30.0	16-21

*Conservative estimate from 4 cells/chain.

Table 1 is a compilation of the published and unpublished references to *G. monilata* in the Banana and Indian rivers along with the available hydrographic data and maximum cell concentrations. Except for the station at Port St. John and the unidentified stations of Howell (1953), the locations of these records are indicated in Fig. 1. The only specific reference to fish kills were by Howell and by B.C.H.D.; however, there is not sufficient evidence to implicate *G. monilata* as the direct cause of death. The fish kill could have been due to oxygen depletion. *G. monilata* has been associated with fish kills along Florida's west coast (Williams and Ingle, 1972), in Pensacola and Mobile bays (Perry et al., 1979) and the Galveston, Texas area (Wardle et al., 1975).

Interestingly, *G. monilata* blooms have had mixed effects in regards to fish kills. For example, Wardle et al. (1975) reported unusual numbers of dead and moribund marine organisms on Galveston Beach associated with a *G. monilata* bloom (1.88×10^6 cells.1^{-1}, 31°C, 33$^o/_{oo}$), while no mortalities were reported by Perry et al. (1979) for Mississippi Sound (1.65×10^7 cells.1^{-1}, 30.0-30.8°C, 24-26$^o/_{oo}$). Both blooms occurred in open waters,
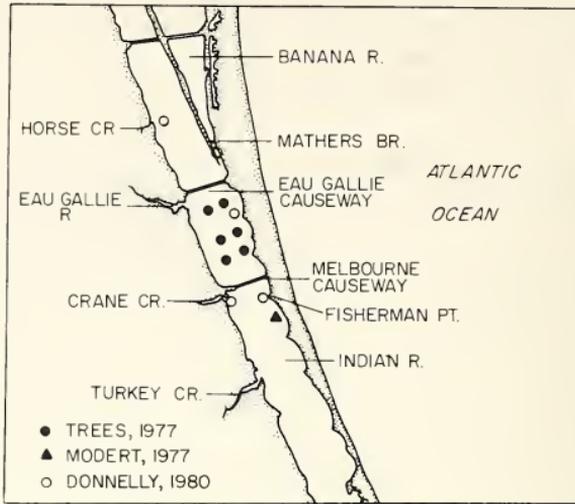
Fig. 1. Distribution of motile *Gonyaulax monilata* cells near Melbourne, Florida.

unlike the lagoonal system of the Indian River. The concentration of *G. monilata* cells (Table 1) reported by Modert (1977) would appear to be sufficient to cause a fish kill though none was reported.

After nearly a year of sampling without collecting any motile cells of *G. monilata*, Donnelly (1980) found low concentrations (Table 1) following the passage of hurricane David in early September 1979. In a 6-mo. study in the same area, David (1978) also did not find motile *G. monilata* cells. This apparent lack of motile cells for months (if not years) supports the belief that benthic resting cysts or hypnozygotes described by Walker and Steidinger (1979) are the only source for the seed population of *G. monilata* blooms in the Indian River lagoon system (Owen and Norris, 1982). Walker and Steidinger (1979) proposed that cysts in Florida waters act as seed beds to initiate *G. monilata* blooms.

LITERATURE CITED

DAVID, J. R. 1978. Net-phytoplankton ecology of the Indian River: the effect of light intensity and temperature upon standing crop during the period October 1977 to April 1978. M.S. thesis, Florida Inst. of Tech., Melbourne.

DONNELLY, P. S. 1980. Dinoflagellate cysts from the Indian River, Florida. M.S. thesis, Florida Inst. of Tech., Melbourne.

Howell, J. F. 1953. *Gonyaulax monilata*, sp. nov., the causative dinoflagellate of a red tide on the east coast of Florida in August-September, 1951. Trans. of the Amer. Microscopical Soc. 72:153-156.

Modert, C. 1977. The effects of ultraviolet radiation on the production rates of natural populations of estuarine phytoplankton. M.S. thesis, Florida Inst. of Tech., Melbourne.

Owen, K. C. and D. R. Norris (1982). Benthic resting cysts of *Gonyaulax monilata* in coastal waters of Mississippi. Fla. Sci. 45:227-233.

Perry, H. M., K. C. Stuck, and H. D. Howse. 1979. First record of a bloom of *Gonyaulax monilata* in coastal waters of Mississippi. Gulf Res. Rep. 6:313-316.

Trees, C. 1977. Suspended solids in a basin of the lagoonal system of Florida. M.S. thesis, Florida Inst. of Tech., Melbourne.

Walker, L., and K. Steidinger. 1979. Sexual reproduction in the toxic dinoflagellate *Gonyaulax monilata*. J. Phycology. 15:312-315.

Wardle, W., S. Ray, and A. Aldrich. 1975. Mortality of marine organisms associated with offshore summer blooms of the toxic dinoflagellate *Gonyaulax monilata* Howell at Galveston, Texas. Pp. 257-263. *In*: LoCicero, V. R. (ed.). Proceedings of the First International Conference on Toxic Dinoflagellate Blooms. Massachusetts Sci. and Tech. Found. Wakefield, Massachusetts.

Williams, J., and R. M. Ingle. 1972. Ecological notes on *Gonyaulax monilata* (Dinophyceae) blooms along the west coast of Florida. Florida Dept. Nat. Resourc. Mar. Res. Lab. Leafl. Ser. Vol. 1, Pt. 1. No. 5.

Academy Symposium

SEDIMENT IN SEAGRASSES NEAR LINK PORT, INDIAN RIVER, FLORIDA

Charles M. Hoskin

Marine Geology Department, Harbor Branch Foundation, Inc.,
R.R. 1, Box 196, Fort Pierce, Florida 33450

Abstract: *Grain size analyses have been made for 34 samples of the upper 5 cm of sediment cores from seagrass beds. Sieves were used for gravel and sand; the SEDIGRAPH was used for silt and clay. Thalassia (13 samples), Halodule (3), Syringodium (3) and bare sand areas (15) within seagrass beds were sampled in the summers of 1979 and 1980. Generally, these sediments are sands, with small admixtures of gravel, silt and clay. The average particle size is about 0.25 mm with grain size modes at 0.3 and 0.1 mm. These sediments are poorly sorted (large standard deviation), positively skewed (excess fine particles) and are leptokurtic (excessive peakedness). Sand content is greater than 90% by weight, and is mostly quartz. Gravel consists of carbonate shells and shell fragments. Mineralogy of the silt fraction is not known, and the clay is judged to be mostly kaolinite from crystal shapes seen in transmission electron microscopy. Comparison of sediment from different species of seagrasses to bare sand areas reveals little difference in terms of grain size characteristics. There are no data available to document seasonal differences. There is a significantly higher content of silt ($\bar{X}$ = 1.33%) in Thalassia sediments than in nearby sandy areas ($\bar{X}$ = 1.01%). Comparison of silt grain size data (62.5 to 3.9 µm) shows that the most abundant particle sizes present in Thalassia sediment are between 15-30 µm. Particle size distribution of silt in nearby sandy areas shows less concentration in this range. Preliminary results from late summer sediment trap measurements give a particle flux of 10-20 g m^{-2} day^{-1} during ordinary weather, which doubled during passage of storm DENNIS. It is not known how much of this flux has come from local resuspension of sediment particles.*